Catena 131 (2015) 14–21

Contents lists available at ScienceDirect

Catena

journal homepage: www.elsevier.com/locate/catena

Recruitment and decay rate of Acacia seedlings in the hyper-arid Arava Valley, Israel

I. Stavi [a,*], R. Shem-Tov [a], Y. Shlomi [a], G. Bel [b], H. Yizhaq [a,b]

[a] Dead Sea & Arava Science Center, Ketura 88840, Israel

[b] Department of Solar Energy and Environmental Physics, Jacob Blaustein Institutes for Desert Research, Ben-Gurion University of the Negev, Sede Boqer Campus, Israel

ARTICLE INFO

Article history:
Received 3 July 2014
Received in revised form 5 March 2015
Accepted 8 March 2015
Available online xxxx

Keywords:
Concentrated flow
Drylands
Geomorphic processes
Fractional exponential decay
Precipitation
Rain storms

ABSTRACT

Acacia trees, including *Acacia pachyceras*, *Acacia raddiana*, and *Acacia tortilis*, constitute some of the main keystone species throughout the hyper-arid Arava Valley of Israel. Several studies performed over the last several decades have revealed drastic changes in the acacia populations, with high mortality rates and low recruitment rates. The objective of this study was to examine the patterns of survivability – through measuring the decay rate – of acacia seedlings during the first year after germination. Following the 2012–2013 rainy season, we measured – over one entire year – the survivability of acacia seedlings in 12 ephemeral rivers (wadis). Data analysis revealed that the main impediment to the recruitment and survival of acacia seedlings is their desiccation, resulting in their mortality. This limiting factor was predominant despite the above-average and well-distributed precipitation during the year of the study. Another, secondary impediment is imposed by erosional and depositional processes under heavy flash floods, resulting in either the uprooting of the seedlings or their burial under deposited soil and fine pebble sediments. Therefore, the novelty of this study stems from the identification, quantification, and modeling of two different mechanisms that determine the decay of acacia seedlings: one with a constant mortality rate that is caused by drying, and the second with a mortality rate that grows with time, which is caused by fluvial processes. The mortality due to drying revealed high fitting to an exponential decay, while the mortality due to fluvial processes closely fits a Gaussian decay function.

1. Introduction

The *Acacia* genus comprises some of the keystone tree species in the hyper-arid Arava Valley of Israel, as well as in other Middle Eastern and North African drylands. During the last several decades, the acacia populations in southern Israel, including *Acacia tortilis*, *Acacia raddiana*, and *Acacia pachyceras*, have experienced dramatic phenological changes, particularly displaying high rates of mortality. The earliest documentation of this trend was released in the mid-1990s, with emphasis on this problem occurring throughout the Arava region (Ashkenazi, 1995). In addition to the high mortality rates, low rates of recruitment have also been highlighted. Previous studies investigated the causes for these low recruitment rates. For example, Ward and Rohner (1997) noted the decrease in the populations of large mammalian herbivores that consume the pods and enhance the germination capacity of seeds through scarification of their hard coats during digestion. Other studies proposed that infestations of insects, such as the bruchid beetle, increase the vulnerability of seeds to predation, resulting in reduced rates of germination (e.g., Or and Ward, 2003). These studies are in accord with a recent research project in several wadis throughout the Arava Valley that revealed little occurrence of young acacias, suggesting a low rate of recruitment (Stavi et al., 2014).

Drastic demographic changes in the acacia populations have also been observed in other Mediterranean drylands, such as in Egypt (Andersen and Krzywinski, 2007) and Tunisia (Noumi and Chaieb, 2012). Yet, despite the extensive research on trends in the acacia populations, very little is known about the mechanisms that affect the survivability of acacia seedlings after germination. Therefore, this study is of wide interest and relevance to the understanding of ecosystem dynamics in African and the Middle Eastern drylands where the *Acacia* genus has been prevalent. Moreover, the importance of acacias in drylands also stems from their positive impact on the physical quality of the soil underneath their canopy, improving the soil–water status and supporting the establishment of understory vegetation (De Boever et al., in press). We believe that the results of this study are not limited to the region in which it took place but that they also shed light on the general mechanisms of the germination and survivability of tree seedlings in dryland riverbeds.

The 2012–2013 rainy season was relatively wet throughout the Arava Valley, reaching a cumulative precipitation rate that was comparatively larger that the long-term inter-annual means (Central Arava R&D website) and that yielded high germination rates of acacia seedlings. The objective of this study was, therefore, to explore the survivability of

* Corresponding author.
E-mail addresses: istavi@adssc.org, istavi@yahoo.com (I. Stavi).

http://dx.doi.org/10.1016/j.catena.2015.03.004

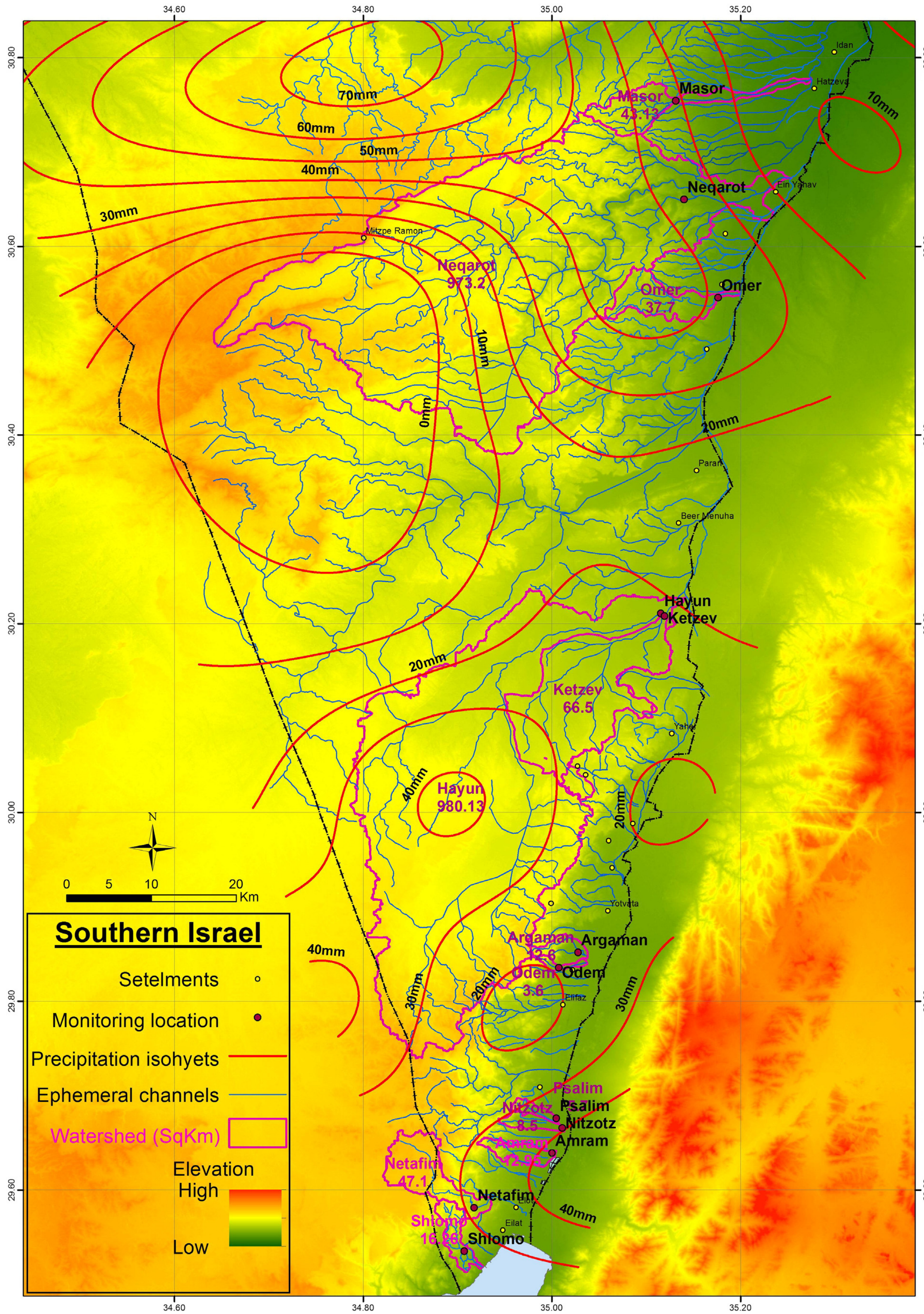

Fig. 1. Map of the study region, with cumulative precipitation isohyets for the 2012–2013 rainy season, and with circumference of the relevant basins. Rainfall data obtained from the Central Arava R&D website. Red dots represent the study's plots. Yellow dots represent rain gauges. (For interpretation of the references to color in this figure legend, the reader is referred to the web version of this article.)

Table 1
Temporal distribution of precipitations (mm) during the rainy season 2012–2013, for selected locations along the Arava Valley.

	Idan	Hatzeva	Ein Yahav	Paran	Yotvata	Eilat
October 2012	0	0.0	0.3	0	0.4	6.4
November 2012	4.8	6.3	5.3	3.8	5	19.4
December 2012	0	0	0	0	0.1	0
January 2013	16.3	9.4	17.5	12.4	8.7	1.8
February 2013	11.5	4.8	11.6	13.8	12.2	16.4
Total	32.6	20.5	34.7	30.0	26.4	44.0

Note: Rain gauges are presented from north (left edge: Idan) to south (right edge: Eilat). Data was obtained from the Central Arava R&D website.

Table 2
Floods' volume in Mm^3, and peak flow discharge (in parentheses) in $m^3 s^{-1}$, during the rainy season 2012–2013 for selected wadis along the study region.

Date	Neqarot	Hayun	Ketzev	Amram	Netafim	Shlomo
01/10/2012	<0.0005 (0.089)	0.237 (58.615)	0.445 (16.3)			
21/10/2012		0.087 (9.267)	0.197 (26.74)		0.009 (5.182)	0.029 (9.08)
23/10/2012	<0.0005 (0.041)					
24/10/2012		0.266 (23.93)	0.038 (5.71)			
09/11/2012						0.024 (9.07)
18/11/2012				0.051 (79.452)		
27/01/2013	0.005 (1.468)					
02/02/2013					0.017 (5.74)	
06/02/2013				0.079 (50.302)		0.022 (6.7)
Cumulative volume	0.006	0.59	0.68	0.13	0.026	0.075

Note: Flood gauges are presented from north (left edge: Neqarot) to south (right edge: Shlomo). Data was obtained from the Water Authority Data Base.

seedlings over one entire year after germination, or more specifically, to quantify and model the decay rate of seedlings throughout this temporal sequence. The study's basic hypothesis was that the decay rate of seedlings is the greatest at the beginning of the dry season and that it follows a decreasing trend along the temporal axis.

2. Materials and methods

2.1. The study region

The Arava Valley is a warm, hyper-arid region, with an approximate elevation of between 100 m below sea level and 200 m above sea level, and running ~160 km from north to south (Fig. 1). The mean daily temperatures in July and December are 31 °C and 15 °C, respectively, at Sapir (the northern edge of the study region), and 32 °C and 16 °C, respectively, at Eilat (the southern edge). The mean relative humidity rates in July and December are 33% and 58%, respectively, at Sapir, and 24% and 47%, respectively, at Eilat (Bitan and Rubin, 1991). The mean cumulative annual precipitation rates during the decade between the rainy season of 2002–2003 and 2011–2012 were 18.1 (±2.3) and 10.1 (±2.9) mm, in the northern and southern Arava Valley, respectively (Meteorological Service website).

Compared with the long-term inter-annual means, the cumulative precipitation rates during the studied rainy season (2012–2013) were 165% (30 mm) and 436% (44 mm) greater in the northern and southern Arava Valley, respectively (Central Arava R&D website). Table 1 shows the temporal distribution of rain events during this season for selected locations throughout the study region. Flood gauges, which have been sparsely installed in the beginning of the 1980s throughout the study region, provided data regarding flood water volume during the 2012–2013 rainy season for some of the wadis (Table 2). For the first half of the following rainy season (October through December 2013), no considerable rainfall event or flood occurred in any of the studied wadis. The only exception to this was a storm that occurred on December 30–31, 2013, resulting in a low-magnitude flood in the Hayun Wadi.

2.2. Specific procedures

In order to best represent the Arava Valley, acacia seedlings were searched in 15 wadis. The features according to which the wadis were selected included: (1) no perturbation by anthropogenic infrastructures (such as earth mining and construction works) that could have altered the natural wadi's water course; (2) the existence of a relatively healthy acacia population; and (3) the occurrence of at least one flood event between October and November 2012. The existence of flood gauges in six of the studied wadis provided data on flood characteristics, including the total volume and peak flow discharge.

At the first stage, in a 1-ha land unit plot of the valley floor of each of the wadis, we searched for “green patches”, indicating the germination of herbaceous vegetation. This was based on the assumption that this germination had occurred in relatively moist zones on the valley floor, which therefore, could also constitute suitable micro-habitats for the germination of acacia seedlings. At the second stage, the green patches were carefully surveyed for acacia seedlings.

Overall, acacia seedlings were located in 12 wadis, including (from south to north): Shlomo, Netafim, Amram, Nitzotz, Psalim, Odem, Argaman, Ketzev, Hayun, Omer, Neqarot, and Masor (Fig. 1 and Table 3). The 1-ha land unit plot was located in the confined stream section – i.e., the section where the floodplain is well-defined due the existence of clear valley walls – of eight of the aforementioned wadis (Shlomo, Netafim, Odem, Ketzev, Hayun, Omer, Neqarot, and Masor), and in the alluvial fans of another four wadis (Amram, Nitzotz, Psalim, and Argaman). The splitting of sampling efforts between the two types of fluvial units was undertaken because of limiting factors, such as anthropogenic perturbations in some of the alluvial fans, and the nonexistence of a clear confined stream section in some other wadis. Regardless, within the 1-ha plots, whenever a seedling was found, its location was marked by a couple of small stones or dry sticks, and a GPS point was recorded to allow us to revisit the same spot. Beginning in January 2013, the wadis were revisited once a month in order to track the existing seedlings, as well as to search for new seedlings.

2.3. Data analysis

The number of seedlings for each wadi was monitored between January and December 2013. Because of their very small initial number of seedlings (<20), some of the wadis were excluded from the analysis. For each of the wadis with a larger number of seedlings, a data analysis was performed, starting from the first month in which no more new seedlings were found. Therefore, the temporal sequence for the analysis started in January for the Amram, Nitzotz, Psalim, Odem, Omer, and Neqarot wadis; in February for the Netafim, Ketzev, Hayun, and Masor wadis; and in March for the Shlomo and Argaman wadis. The temporal sequence (monthly records of the number of seedlings) for the analysis was terminated in the last month with the number of seedlings larger than zero. The data from all the wadis were combined and used for analyzing the mortality of the entire seedling population. In order to fit the mortality curves to a mathematical function, we first normalized the data for each wadi as follows: (i) we subtracted from the number of live seedlings, at any time, the number of seedlings that were still alive at the last survey (the final number of seedlings); (ii) the shifted numbers (the series resulting from step i) were divided by the difference between the initial number of live seedlings and the final number. This normalization procedure ensured that each normalized

Table 3
Acacia seedling distribution, by wadi and month.

Wadi	Shlomo	Netafim	Amram	Nitzotz	Psalim	Odem	Argaman	Ketzev	Hayun	Omer	Neqarot	Masor	Total
Longitude (°)	34.9072	34.9176	35.0002	35.0109	35.0047	35.0072	35.0276	35.1194	35.1155	35.1758	35.1398	35.1312	–
Latitude (°)	29.5349	29.5810	29.6389	29.6656	29.6759	29.8355	29.8518	30.2083	30.2112	30.5457	30.6498	30.7545	–
Cumulative floods (mm^3)	0.0750	0.0260	0.1300	NA	NA	NA	NA	0.6800	0.5900	NA	0.006	NA	–
Green patches' area (ha)	0.047	0.048	0.041	0.085	0.055	0.028	0.128	0.052	0.052	0.057	0.185	0.063	0.900
January	63	10	29	14	47	6	180	106	70	153	69	16	763
February	39	10 + 3	17	6	5	3	129	101 + 14	65 + 41	5	61	16 + 12	457 + 70
March	45*	13	16	5	5	3	122 + 4	71	106	5	57	15	463 + 4
April	42	11	14	2	4	3	100	44	95	5	50	4	374
May	32	8	4	1	1	3	64	10	54	3	32	3	215
June	17	7	2	0	0	1	16	7	40	1	20	3	114
July	6	3	1	0	0	1	4	5	9	1	15	3	48
August	3	3	1	0	0	1	2	3	3	0	13	0	29
September	1	3	0	0	0	1	2	3	3	0	12	0	25
October	1	3	0	0	0	1	1	3	3	0	12	0	24
November	1	3	0	0	0	1	1	3	2	0	12	0	23
December	1	3	0	0	0	1	1	2	2	0	11	0	21

Note: NA — not available. *of these, 6 buried sprouts re-emerged from the covering sediments.

series started at 1 and ended at 0. Three functions – exponential ($f(t)$) (Eq. (1)),Gaussian ($g(t)$) (Eq. (2)), and fractional exponential ($h(t)$) (Eq. (3)) – were used for modeling the decay rate of the normalized number of seedlings:

$$f(t) = \exp(-bt) \tag{1}$$

$$g(t) = \exp\left(-(bt)^2\right) \tag{2}$$

$$h(t) = \exp(-(bt)^a) \tag{3}$$

where a and b are coefficients to be determined from the curve fitting procedure. In all three functions, $1/b$ provides the characteristic time scale of the mortality process. The coefficient in front of the exponent was set to unity in all of the functions to ensure that the initial number of seedlings is equal to the observed number. Note that the exponential and the Gaussian functions have one degree of freedom, whereas two parameters are needed to determine the fitting of the fractional exponent function. Thus, it is expected that the fit to the fractional exponent function will be better. The exponential function demonstrates a decay process with a constant (b) rate, which is named the exponential decay constant and describes a population number that decreases at a rate proportional to its current value. Mathematically, the exponential decay function is the solution of the first order linear differential equation (Eq. (4)):

$$\frac{dN}{dt} = -bN, \tag{4}$$

where N is the number of seedlings at time t, and b is the exponential decay constant, which is the time at which the population of surviving seedlings is reduced to $1/e = 0.368$ times its initial value. Exponential decay implies that the probability of a seedling to die is independent of how long it has survived so far.

The Gaussian function is the solution of the following first order linear differential (Eq. (5)):

$$\frac{dN}{dt} = -2b^2tN. \tag{5}$$

The Gaussian function demonstrates a decay process in which the rate increases linearly with time (the term $2b^2t$ in Eq. (5)), in contrast to the exponential decay where the rate is constant (the term b in Eq. (4)).

The fractional exponent function depicts the general case in which the power a can be any real positive number. The fractional exponent, with $0 < a < 1$, is known as a stretched exponent, whereas for $a > 1$, it is termed a compressed exponential function. At the same time, $a = 1$ corresponds to the usual exponential function, and $a = 2$ corresponds to the Gaussian function. Thus, $h(t)$ can be considered a generalization of the exponential function. The fractional exponent function is the solution of the following first order linear differential (Eq. (6)):

$$\frac{dN}{dt} = (\gamma t)^{a-1}N \tag{6}$$

where $\gamma \equiv (ab)^{\frac{1}{a-1}}$.

These three functions were chosen based on their simplicity and fitness in analyzing datasets that describe demographic changes of populations. MATLAB statistical tools were used for the data analysis and fitting procedure.

In addition, the drainage area for each of the wadis was calculated using GIS GRASS (2012). Drainage points were determined at the most downstream spot among the sampled trees in each wadi. Elevation data were obtained from the ASTER Global Digital Elevation Model (ASTER GDEM). The data were of resolution 1 arc-sec. Using GRASSGIS watershed modules, flow accumulation and flow direction grids, as well as a stream network, were obtained. Next, each of the determined outlet points was utilized for delineating the basin draining at that point. The basins were then vectorized, and their area was calculated. Then, Pearson correlation coefficients were calculated to examine the relationships between basin size and flood characteristics (for the wadis that contain the rain gauges).

3. Results and discussion

In drylands, due to the relatively higher moisture content in streams than in the surrounding uplands, the abundance and diversity of vegetation and wildlife on the riverbeds are considerably higher. As a response to short-duration high-intensity precipitation events, the (concentrated) flow in these ephemeral streams most often occurs as flash floods, usually lasting only minutes or hours (Levick et al., 2008). Due to high runoff coefficients and the dominance of Hortonian overland flow in runoff generation, the hydrographs of such storms are characterized by a steep rising to the peak flow, followed by a much longer recession phase (Dick et al., 1997). The unconsolidated alluvium, comprised of gravel, a high percentage of sand and silt, and a small percentage of cohesive clays (Vyverberg, 2010), coupled with the high velocity turbulent flash flows (Levick et al., 2008), results in the high mobility of sediments during these floods. Therefore, bedload transport rates and suspended sediment concentrations are generally high in dryland streams (Vyverberg, 2010).

In January 2013, a total of 763 seedlings were located throughout the study region. In February 2013, 457 of these were still alive. A heavy rainstorm occurred between these two surveys throughout the Arava Valley (as shown in Table 1), resulting in floods in several wadis across the region. Therefore, the seedling mortality of 40% between the January and February surveys suggests that flash floods – with a high bedload transport capacity (Levick et al., 2008; Vyverberg, 2010) – may inhibit the recruitment of acacia trees. In addition to these 457 seedlings, 70 new seedlings were located during the February survey. In the March survey, of the previously observed 527 seedlings, 463 were still alive, and additional four new seedlings were located. After this, no more new seedlings were located, and the total number of live seedlings decreased continuously. Of the total numbers of seedlings, the normalized percentages in the confined stream section's plots and in the alluvial fan's plots were 78.8% and 21.2%, respectively, in January; 82.7% and 17.3%, respectively, in February; and 80.8% and 19.2%, respectively, in March. At the end of 2013, the normalized percentages of seedlings were 97.6% and 2.4%, respectively. To some extent, the sharp decrease in the overall percentage of seedlings in the alluvial fans throughout the studied period could be related to the absence of pebble cover (Fig. 2). This is assumed to decrease the soil infiltration capacity and the wetting front and to increase the water evaporation rate, exacerbating water stress for the seedlings. This is in contrast to the relatively high pebble cover in the confined stream sections (Fig. 3), assumed to increase infiltration and the wetting front, and to decrease evaporation loss (see: Li, 2003).

In addition to ground surface cover, microtopography is also expected to determine the availability of water for the vegetation (Stavi et al., 2014), supporting its growth in depressions, where water is accumulated. In addition, the location of vegetation on bars could also be perceived as effective in protecting the plants from devastating floods and sediment deposition. However, most of the seedlings were located on relatively plane ground surfaces, some others on bars, and only a few in depressions. Therefore, we cannot assess the effects of microtopography on seedling germination and survivability in drylands.

The results of the curve fitting analysis are shown in Fig. 4 and in Table 4. Overall, the three functions (exponential, Gaussian, and fractional exponential) fit the data well. The curve fitting showed that in some wadis, the mortality rate grew with time (Gaussian fit), while in others, it was almost independent of time and remained constant (exponential fit). For example, in the Shlomo wadi, the mortality rate grew with time, and therefore, both the Gaussian and the fractional exponential ($a = 2.538$) functions provided an excellent fit, while the exponential function, which corresponds to a constant mortality rate, did not fit the data well. On the other hand, in the Amram Wadi, the mortality rate was almost constant, and therefore, the Gaussian function did not fit the data as well as did the exponential function. In this wadi, the fractional exponential function was very similar to the exponential function ($a = 1.1630$). The relevant data (provided by the rain gauges)

Fig. 2. Amram Wadi. Note the exposed soil surface.

Fig. 3. Shlomo Wadi. Note the full pebble cover of the surface.

on extreme flood characteristics – after seedling germination – revealed data for only one flood event, in the Amram Wadi, and indicated an extreme peak flow of 50.3 $m^3 s^{-1}$, which took place in February (Table 2). Unexpectedly, this event did not increase the mortality rate.

The total number of acacia seedlings throughout the studied temporal sequence is well demonstrated by the exponential decay ($R^2 = 0.9621$). Therefore, for the entire dataset, the mortality rate was almost constant, implying that the mortality, which is proportional to the number of seedlings, was high at the beginning and decreased as the number of seedlings declined. The exponential constant of decay (b) indicates the decay rate. As shown in Table 4, the slowest decay was reported for the Neqarot Wadi (where b is the smallest for each of the three functions). At the same time, the fastest decay (largest b) was observed in the Omer Wadi. This extremely fast mortality process required special attention. During the January survey in the Omer Wadi, 153 seedlings were located in its channel. During this wadi's February survey, signs of a heavy flood were found across the channel, and 148 of these 153 seedlings had disappeared. It seems that the rainstorm of February 5th, which occurred six days before this survey, generated a heavy flash flood, removing the mineral material and uprooting acacia seedlings from the wadi's valley floor. This was also supported by several observations across the wadi's channel, revealing recent exposures of extensive areas. Unfortunately, the absence of a flood gauge in this wadi prevented us from studying the specific characteristics (e.g., flow duration and peak flow) of this flood event. Yet, it can be assumed that the peak flow of this flood was extremely high, resulting in a very high rate of bedload transport, with the associated uprooting of seedlings from the channel bed. A similar trend of a sharp decrease in the number of seedlings, though at a much lower magnitude, was also observed in the Psalim Wadi. However, this could not be attributed to floods, as no considerable rainstorm occurred between the first and second surveys in the Psalim region.

Regardless, the obtained results – suggesting that the young seedlings on the floors of the wadis are put at risk of uprooting because of the concentrated erosional processes – are in accord with studies from the southwestern United States, which revealed that flash floods may jeopardize the existing vegetation on the floors of ephemeral rivers (Levick et al., 2008; Vyverberg, 2010). Particularly, this is in accord with Andersen and Krzywinski (2007) who reported that in the hyper-arid Egyptian Eastern Desert, *A. tortilis* trees that grow in proximity to ephemeral streams are at risk of being uprooted by floods. Also, on the floors of some of the wadis, we located seedlings with partially exposed roots, indicating the removal of topsoil by erosion. For example, five days after the February 5th rainstorm, the roots of some seedlings, previously located in the Netafim and Amram Wadis, were almost fully exposed due to soil erosion (Fig. 5). In March, most of these

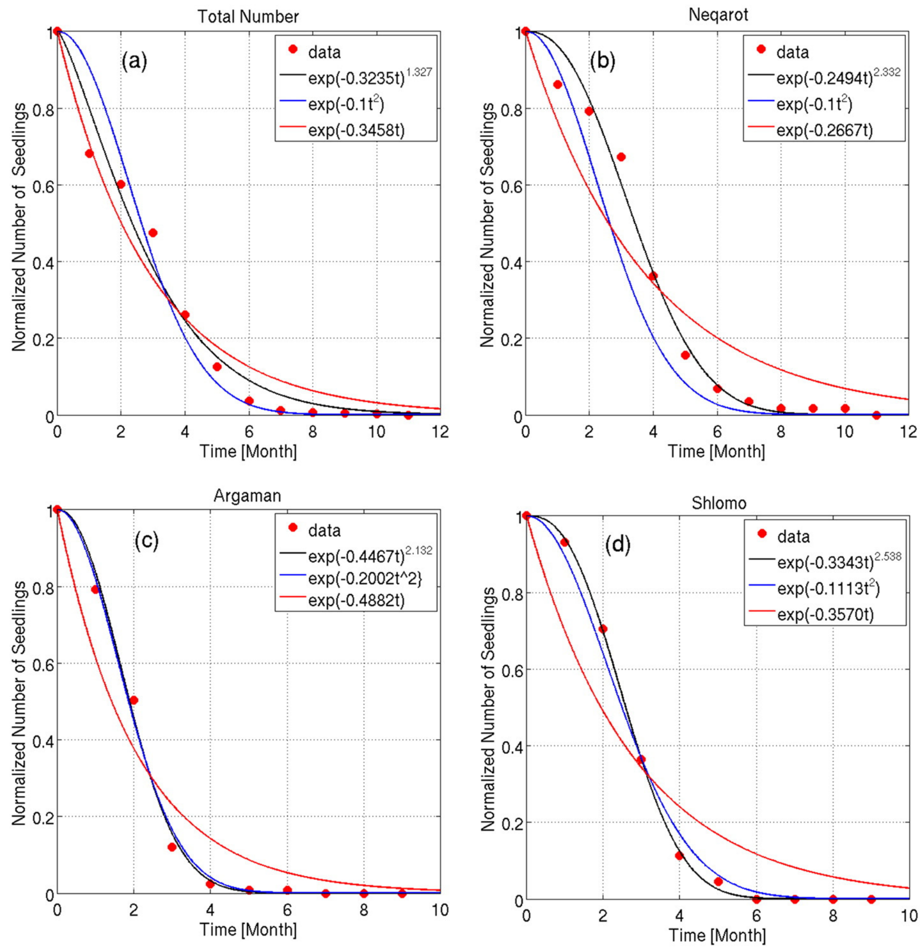

Fig. 4. Curve fitting functions (exponential, Gaussian, and fractional exponential) for the total number of seedlings (a), Neqarot Wadi (b), Argaman Wadi (c), and Shlomo Wadi (d). More details of the fittings are available in Table 4.

seedlings were dead (and in April, all of these seedlings were dead), presumably due to inaccessible soil–water for the roots.

In addition to the direct erosion effect, the obtained results revealed that the deposition of sediments also affects the survivability of seedlings in the channels. Following the storm event on February 5th, several seedlings, located on the valley floors, were buried alive underneath sediments. Five days after this rainstorm, we located 20 seedlings in the Shlomo Wadi and an additional 11 seedlings in the Amram Wadi that were partially (Fig. 6) or fully (Fig. 7) buried under deposited sediments. Presumably, the burial of seedlings by soil or fine pebble sediments indicates the occurrence of relatively low-energy floods, which enabled the predominance of depositional processes over erosional ones. This is in accord with the location of these seedlings in an alluvial fan (of the Amram Wadi: Fig. 2) and a secondary channel (of the Shlomo Wadi: Fig. 3), with the presumed lower runoff energy (see: Brady and Vyverberg, 2013). In the March survey, we located, in the Shlomo Wadi, six previously buried seedlings reemerging out of the fine pebble sediment cover. Despite the unknown conditions under which the buried seedlings can reemerge from the deposited sediments, it can be assumed that if seedlings are buried underneath a relatively deep layer of sediments, then some of them may die due to a prolonged inhibition of sunlight.

The frequency and magnitude of flash floods could have seemingly been expected to be inversely related to the basin size. However,

Table 4
Exponential, Gaussian, and fractional exponential curve fitting coefficients, by wadi.

Location	R^2 exponential	R^2 Gaussian	R^2 fractional exponential	*b* coefficient exponential	*b* coefficient Gaussian	*b* coefficient fractional exponential	*a* coefficient fractional exponential
Shlomo	0.8964	0.9940	0.9996	0.3570	0.3336	0.3343	2.5380
Amram	0.9199	0.8630	0.9244	0.4153	0.3624	0.3992	1.1630
Psalim	0.9857	0.9834	0.9936	2.2530	1.5620	4.0000	0.5096
Argaman	0.9349	0.9953	0.9957	0.4882	0.4474	0.4467	2.1320
Ketzev	0.9810	0.9779	0.9925	0.5974	0.5496	0.5608	1.3840
Omer	0.9982	0.9981	0.9984	3.5820	1.9068	6.0000	0.6743
Neqarot	0.8990	0.9870	0.9893	0.2677	0.2497	0.2494	2.3320
Masor	0.9712	0.9998	1.0000	0.9772	0.8625	0.8650	2.1330
All sites	0.9621	0.9501	0.9768	0.3458	0.3087	0.3235	1.3270

Fig. 5. An almost fully uprooted acacia seedling. Notice the exposed ~9-cm length of root system. Photo was taken (from above, in a parallel position to the ground surface) in the Shlomo Wadi, five days after a flood event.

Fig. 7. An acacia seedling exposed after excavation in soil. The whole seedling (3-cm height) was covered with sediments, and its location was identified by the marking stones around it. Photo was taken in the Shlomo Wadi, five days after a flood event.

examining the relationships of the Pearson correlation coefficients between basin size and each of the flood characteristics, including frequency (number), cumulative volume, and mean peak discharge, throughout the studied year, revealed a strong relationship ($r > 0.50$) only regarding the frequency. Actually, this relationship was positive, showing increased frequency with the increase in basin size. To some extent, the absence of the effect of basin size on flood characteristics is in accordance with Goodrich et al. (1997), who reported that in southwestern Arizona, the runoff/rainfall rate becomes more non-linear with increasing watershed size because of the increasing importance of ephemeral stream channel transmission losses and the partial storm area coverage. Also, this is in accord with Stavi et al. (2014) who revealed no effect of basin area on the mortality rate of adult acacias across the Arava Valley, suggesting that the mortality of trees is determined by the smaller-scale heterogeneity of lithologic, pedogenic, and fluvial characteristics rather than by the large-scale topographic background.

Fig. 6. An acacia seedling partially covered with sediments. Photo was taken in the Amram Wadi, five days after a flood event.

The results showed that different wadis experienced different levels of dependence between the mortality rate and the time passed since germination, ranging from a weak dependence in the Amram Wadi to a very strong dependence in the Shlomo Wadi. The overall mortality trend across the study region revealed a constant rate, resulting in an exponential decay of the studied population, and negating the study's hypothesis. This research demonstrates the need to employ large-scale sampling and monitoring schemes in order to effectively represent the prevailing combinations of physio-biological conditions. This may be particularly relevant for drylands, where climatic conditions are severe and precipitation regimes are highly erratic in space and time. Future research should focus on the actual relationships between flood characteristics and acacia seedling recruitment. Particularly, high-resolution (spatial and temporal) data obtained from flood gauges could provide information on flow characteristics, including peak discharge, duration, and recession rate, increasing the understanding of their effects on the seedlings. Also, site-specific (seedling-spot) conditions – such as stratigraphy and particle-size composition – that determine water accessibility for seedlings would have to be thoroughly studied in the future, providing important information regarding recruitment of acacia seedlings in hyper-arid environments.

4. Conclusions

According to this study, the desiccation of seedlings is the major cause of their mortality. In addition, geomorphic processes, i.e., soil erosion with the associated uprooting of seedlings, and burial by deposited soil and fine pebble sediments, were also observed to limit the survivability of many seedlings. The two effects cause considerably different temporal patterns of mortality. The overall trend of seedlings survival during the first year after germination throughout the Arava Valley fits well an exponential decay curve. Further studies are needed in order to explore, over the long term, the patterns of seedling recruitment and survival of the several species of the *Acacia* genus found in southern Israel, as well as in other Middle Eastern and North African drylands. Particularly, future efforts should be focused on the site-specific characterization of soil features that determine water accessibility for the seedlings. These studies should be implemented over several consecutive years, with the aim of improving the understanding of long-term trends that affect the demography of acacia populations.

Acknowledgments

The study was partially funded by the ICA in Israel (the JCA Charitable Foundation). The authors kindly acknowledge the very helpful commentaries on a previous version of the manuscript by two anonymous reviewers.

References

Andersen, G.L., Krzywinski, K., 2007. Mortality, recruitment and change of desert tree populations in a hyper-arid environment. PLoS ONE 2, e208. http://dx.doi.org/10.1371/journal.pone.0000208.

Ashkenazi, S., 1995. Acacia Trees in the Negev and Arava, Israel — A Review Following Reported Large-scale Mortality. Hakeren Hakayemet LeIsrael, Jerusalem.

ASTER GDEM, M. Maintained by the NASA Land Processes Distributed Active Archive Center (LP DAAC). https://lpdaac.usgs.gov.

Bitan, A., Rubin, S., 1991. Climatic Atlas of Israel for Physical and Environmental Planning and Design. 3rd ed. Ramot Press, Tel Aviv.

Brady, R.H., Vyverberg, K., 2013. Methods to Describe and Delineate Episodic Stream Processes on Arid Landscapes for Permitting Utility-scale Solar Power Plants. California Energy Commission (Publication Number CEC-500-2014-013. http://www.energy.ca.gov/2014publications/CEC-500-2014-013/CEC-500-2014-013-APG.pdf).

Central Arava R&D website: http://www.arava.co.il/haklaut/mop/clim/weatherforecast_new.htm.

De Boever, M., Gabriels, D., Ouessar, M., Cornelis, W., 2014. Influence of acacia trees on near-surface soil hydraulic properties in arid Tunisia. Land Degrad. Dev. http://dx.doi.org/10.1002/ldr.2302 (in press).

Dick, G.S., Anderson, R.S., Sampson, D.E., 1997. Controls on flash flood magnitude and hydrograph shape, Upper Blue Hills badlands, Utah. Geology 25, 45–48.

GIS GRASS, 2012. Grass Development Team, Geographic Resources Analysis Support System Software. Open Source Geospatial Foundation Project (http://grass.osgeo.org).

Goodrich, D.C., Lane, L.J., Shillito, R.M., Miller, S.N., Syed, K.H., Woolhiser, D.A., 1997. Linearity of basin response as a function of scale in a semiarid watershed. Water Resour. Res. 33, 2951–2965.

Levick, L., Fonseca, J., Goodrich, D., Hernandez, M., Semmens, D., Stromberg, J., Leidy, R., Scianni, M., Guertin, D.P., Tluczek, M., Kepner, W., 2008. The ecological and hydrological significance of ephemeral and intermittent streams in the arid and semi-arid American Southwest. U.S. Environmental Protection Agency and USDA/ARS Southwest Watershed Research Center (EPA/600/R-08/134, ARS/233046, 116 pp.).

Li, X.Y., 2003. Gravel–sand mulch for soil and water conservation in the semiarid loess region of northwest China. Catena 52, 105–127. http://dx.doi.org/10.1016/S0341-8162(02)00181-9.

Meteorological Service website: http://data.gov.il/ims.

Noumi, Z., Chaieb, M., 2012. Dynamics of *Acacia tortilis* (Forssk.) Hayne subsp. *raddiana* (Savi) Brenan in arid zones of Tunisia. Acta Bot. Gall. 159, 121–126. http://dx.doi.org/10.1080/12538078.2012.671665.

Or, K., Ward, D., 2003. Three-way interactions between acacia, large mammalian herbivores and bruchid beetles — a review. Afr. J. Ecol. 41, 257–265. http://dx.doi.org/10.1046/j.1365-2028.2003.00451.x.

Stavi, I., Silver, M., Avni, Y., 2014. Latitude, basin size, and microhabitat effects on the viability of Acacia trees in the Negev and Arava, Israel. Catena 114, 149–156. http://dx.doi.org/10.1016/j.catena.2013.10.006.

Vyverberg, K., 2010. A Review of Stream Processes and Forms in Dryland Watersheds. California Department of Fish and Game, Sacramento, CA (https://nrm.dfg.ca.gov/FileHandler.ashx?DocumentID=25779).

Ward, D., Rohner, C., 1997. Anthropogenic causes of high mortality and low recruitment in three acacia tree taxa in the Negev desert, Israel. Biodivers. Conserv. 6, 877–893. http://dx.doi.org/10.1023/B:BIOC.0000010408.90955.48.

Water Authority Data Base. http://www.water.gov.il/Hebrew/ProfessionalInfoAndData/Data-Hidrologeime/Pages/default.aspx.